Shear-Wave Elastography for the Estimation of Liver Fibrosis in Chronic Liver Disease: Determining Accuracy and Ideal Site for Measurement[1]

Anthony E. Samir, MD, MPH
Manish Dhyani, MBBS
Abhinav Vij, MBBS, MPH
Atul K. Bhan, MBBS, MD
Elkan F. Halpern, PhD
Jorge Méndez-Navarro, MD
Kathleen E. Corey, MD, MPH
Raymond T. Chung, MD

Purpose: To evaluate the accuracy of shear-wave elastography (SWE) for staging liver fibrosis in patients with diffuse liver disease (including patients with hepatitis C virus [HCV]) and to determine the relative accuracy of SWE measurements obtained from different hepatic acquisition sites for staging liver fibrosis.

Materials and Methods: The institutional review board approved this single-institution prospective study, which was performed between January 2010 and March 2013 in 136 consecutive patients who underwent SWE before their scheduled liver biopsy (age range, 18–76 years; mean age, 49 years; 70 men, 66 women). Informed consent was obtained from all patients. SWE measurements were obtained at four sites in the liver. Biopsy specimens were reviewed in a blinded manner by a pathologist using METAVIR criteria. SWE measurements and biopsy results were compared by using the Spearman correlation and receiver operating characteristic (ROC) curve analysis.

Results: SWE values obtained at the upper right lobe showed the highest correlation with estimation of fibrosis ($r = 0.41$, $P < .001$). Inflammation and steatosis did not show any correlation with SWE values except for values from the left lobe, which showed correlation with steatosis ($r = 0.24$, $P = .004$). The area under the ROC curve (AUC) in the differentiation of stage F2 fibrosis or greater, stage F3 fibrosis or greater, and stage F4 fibrosis was 0.77 (95% confidence interval [CI]: 0.68, 0.86), 0.82 (95% CI: 0.75, 0.91), and 0.82 (95% CI: 0.70, 0.95), respectively, for all subjects who underwent liver biopsy. The corresponding AUCs for the subset of patients with HCV were 0.80 (95% CI: 0.67, 0.92), 0.82 (95% CI: 0.70, 0.95), and 0.89 (95% CI: 0.73, 1.00). The adjusted AUCs for differentiating stage F2 or greater fibrosis in patients with chronic liver disease and those with HCV were 0.84 and 0.87, respectively.

Conclusion: SWE estimates of liver stiffness obtained from the right upper lobe showed the best correlation with liver fibrosis severity and can potentially be used as a noninvasive test to differentiate intermediate degrees of liver fibrosis in patients with liver disease.

Online supplemental material is available for this article.

[1] From the Department of Radiology (A.E.S., M.D.), Department of Pathology (A.K.B.), Institute for Technology Assessment (E.F.H.), and Department of Hepatology, Liver and GI Division, Department of Medicine (K.E.C., R.T.C.), Massachusetts General Hospital, Harvard Medical School, 55 Fruit St, Boston, MA 02114; Department of Radiology, Bryn Mawr Hospital, Bryn Mawr, Pa (A.V.); and Department of Gastroenterology, National Medical Center, Hospital de Especialidades, CMN Siglo XXI, IMSS, Mexico City, Mexico (J.M.N.). Received April 15, 2014; revision requested May 27; revision received July 8; accepted July 25; final version accepted August 13. **Address correspondence to** A.E.S. (e-mail: *asamir@partners.org*).

The prevalence of chronic liver disease (CLD) in the United States between 2005 and 2008 was estimated to be as high as 14.8% (1), with as many as 150000 new cases diagnosed each year (2)—20% of which had cirrhosis at presentation. The multiple causes of CLD follow a common pathway of progressive liver fibrosis, ultimately culminating in cirrhosis. These include hepatitis C virus (HCV), hepatitis B virus, nonalcoholic fatty liver disease, and alcoholic liver disease (3). Although the prevalence of major causes of CLD remains stable, data from the National Health and Nutrition Examination Surveys show that nonalcoholic fatty liver disease will be a substantial burden on the prevalence of CLD in the United States (1). Advanced fibrosis, cirrhosis, and hepatocellular carcinoma develop in about 17%–55% of patients with HCV and 20%–40% of those with hepatitis B virus and nonalcoholic steatohepatitis (4–6). Although early fibrosis has been shown to be partly reversible, cirrhosis is, by definition, irreversible. Hence, the goal of CLD management is to prevent progression to cirrhosis and attempt reversal of early fibrosis. Liver biopsy is currently the standard of reference for the evaluation of fibrosis in patients with known liver disease. However, liver biopsy is invasive, associated with morbidity, and expensive (7). The accuracy of liver biopsy is also limited by interobserver variability and sampling error (7). The high cost and limited patient acceptance make it impractical to repeatedly perform liver biopsy for the long-term monitoring of CLD.

As a result, there has been a search for alternate noninvasive methods for diagnosing and staging liver fibrosis (8). Surrogate blood markers and imaging techniques have been shown to help predict liver fibrosis stage with varying degrees of accuracy. Imaging techniques used thus far have included morphologic analysis, computed tomographic (CT) perfusion analysis (9), magnetic resonance (MR) perfusion analysis (10), water diffusion imaging (11,12), and elastography. Ultrasonographic (US) elastography and MR elastography have both shown promising results in several clinical studies (11,13–15), with US-based elastography providing the additional advantage of real-time imaging and lower cost. Transient elastography, a vibroacoustic nonimaging technology, and acoustic radiation force imaging, which is an imaging-based technology, have both been shown to be highly accurate for the diagnosis of cirrhosis and of intermediate accuracy for the differentiation of mild and moderate hepatic fibrosis (13–15). Shear-wave elastography (SWE) uses measurement of acoustically generated tissue shear wave propagation speeds to derive estimates of liver stiffness, with the advantage of simultaneous anatomic B-mode US imaging (16). This allows selection of a liver parenchymal region of interest devoid of blood vessels or focal lesions for analysis.

The literature specifically assessing the utility of noninvasive assessment of CLD with use of SWE technology is limited, and the ideal site for SWE evaluation has not yet been determined. The purpose of this cross-sectional study was to evaluate the accuracy of SWE for staging liver fibrosis in patients with diffuse liver disease (including patients with HCV) and to determine the relative accuracy of SWE measurements obtained from different hepatic acquisition sites for staging liver fibrosis.

Advances in Knowledge

- Estimates of liver stiffness with shear-wave elastography (SWE) showed the highest correlation with the stage of liver fibrosis when obtained in the upper right lobe of the liver ($r = 0.41$, $P < .001$); values obtained in the left lobe of the liver did not correlate with the fibrosis stage at liver biopsy ($r = 0.16$, $P = .06$).
- SWE shows a high diagnostic accuracy in differentiating lower stages of fibrosis (F0, F1) from higher stages of fibrosis (F2, F3, F4), with an area under the receiver operating characteristic curve (AUC) of 0.77; when adjusted for spectrum bias, the AUC is 0.84.

Implication for Patient Care

- SWE can be used to noninvasively stage liver fibrosis in patients with diffuse liver disease and in some clinical circumstances may replace liver biopsy for this purpose.

Materials and Methods

SuperSonic Imagine (Aix-en-Provence, France) supported the study by loaning an Aixplorer system to the investigators. The authors had control of the data and the information submitted for publication.

Design Overview and Study Population

This prospective single-institution study was approved by the institutional review board and was compliant with the Health Insurance Portability and Accountability Act. Patients known to have or suspected of having diffuse liver disease who were scheduled for US-guided nonfocal liver biopsy in the interventional radiology department were eligible for the study.

Published online before print
10.1148/radiol.14140839 **Content codes:** GI US

Radiology 2015; 274:888–896

Abbreviations:
AUC = area under the ROC curve
CI = confidence interval
CLD = chronic liver disease
DANA = difference between the mean fibrosis stage of advanced fibrosis and the mean fibrosis stage of nonadvanced fibrosis
HCV = hepatitis C virus
ROC = receiver operating characteristic
SWE = shear-wave elastography

Author contributions:
Guarantors of integrity of entire study, A.E.S., M.D.; study concepts/study design or data acquisition or data analysis/interpretation, all authors; manuscript drafting or manuscript revision for important intellectual content, all authors; manuscript final version approval, all authors; agrees to ensure any questions related to the work are appropriately resolved, all authors; literature research, A.E.S., M.D., A.V., J.M.N., K.E.C.; clinical studies, A.E.S., A.V., A.K.B., J.M.N., K.E.C., R.T.C.; statistical analysis, M.D., E.F.H.; and manuscript editing, A.E.S., M.D., A.V., R.T.C.

Funding:
R.T.C. supported by the National Institutes of Health (grant DK078772).

Conflicts of interest are listed at the end of this article.

Figure 1

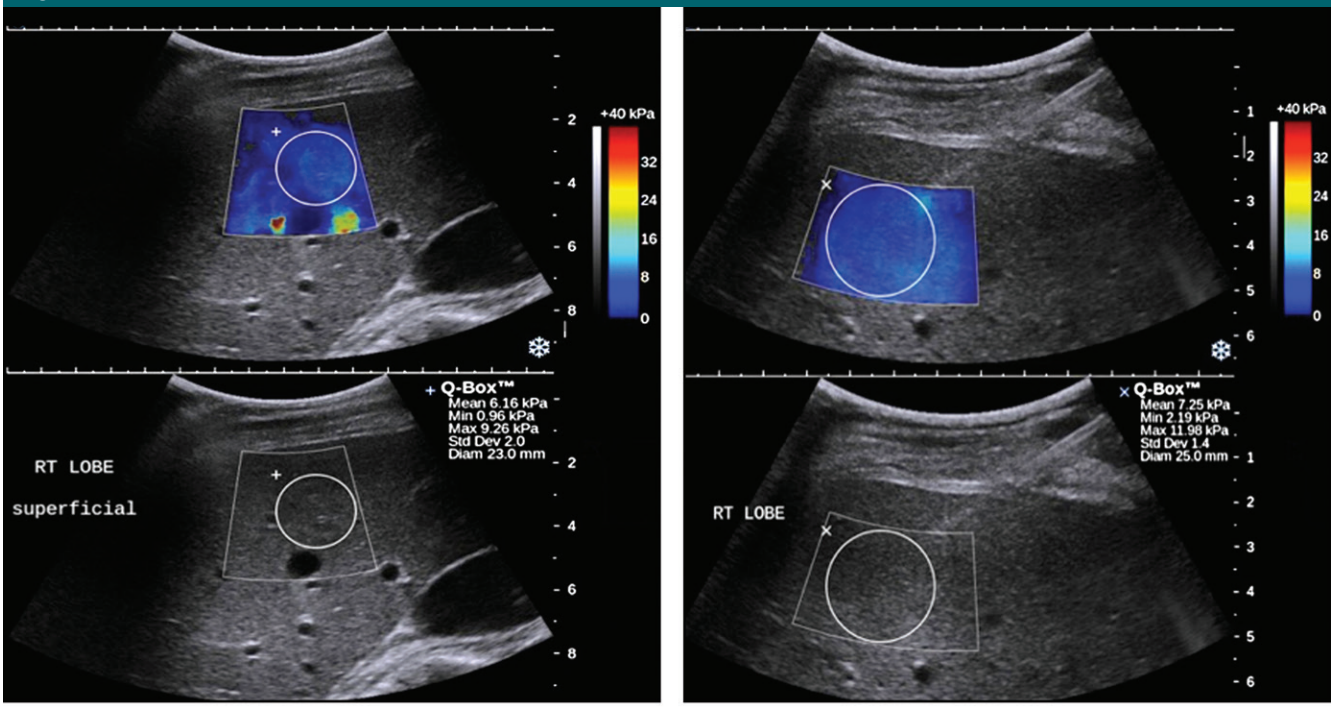

a. b.

Figure 1: Examples of SWE values obtained from offline quantification by placing a region of interest on elastograms obtained **(a)** in upper right lobe and **(b)** at biopsy site with needle in position. Both regions of interest were placed in an area devoid of blood vessels.

Patients younger than 18 years were not included in the study. Informed consent was obtained from patients who fulfilled the inclusion criteria before the liver biopsy procedure. Under institutional review board approval, it was mandatory that a physician who did not obtain consent and/or perform the clinical liver biopsy obtain informed consent for participation in the research study. All subjects underwent a SWE examination performed by a sonographer with more than 5 years of experience. Nonfocal liver biopsies were subsequently performed under US guidance. Pathologic assessment of liver biopsies with use of the METAVIR histopathology scoring system was used as the standard of reference.

SWE Examination

SWE was performed by using the Aixplorer US system (SuperSonic Imagine) with a convex broadband probe (SC6–1, SuperSonic Imagine). The technology measures the speed of shear wave propagation (16), which is then used to compute tissue stiffness, also known as the Young modulus of elasticity, in kilopascals. These quantitative values are also mapped as a color-coded two-dimensional SWE image of tissue stiffness, which is simultaneously generated with conventional B-mode images.

SWE was performed by one sonographer with 16 years of experience immediately before liver biopsy in the interventional radiology US suite. Each SWE acquisition comprises 20 sequential measurements recorded in the form of a cine clip. Before biopsy, three 20-measurement elastographic cine clips were obtained at each of the following locations in the liver: *(a)* left lobe, *(b)* upper right lobe, and *(c)* lower right lobe. Patients were not sedated. Upper right lobe measurements were defined as measurements obtained at a depth of less than 5 cm from the skin surface. Upper right lobe measurements were obtained by means of an intercostal acoustic window, whereas lower right lobe measurements were either intercostal or subcostal. Before biopsy sampling, a fourth set of three cine loop elastograms was acquired from the region of the liver that was selected as the biopsy site with the biopsy needle in position (Fig 1). Hence, a total of 12 SWE cine loops, comprising 240 distinct elastographic measurements, were acquired from four sites. After the biopsy, we performed image postprocessing at a dedicated workstation. On this dedicated workstation, a postdoctoral research fellow (M.D.) with 1 year of experience in elastography placed all regions of interest within the SWE image with a qualitative image scale extending from 0 to 40 kPa. The largest possible region of interest (range, 10–30 mm^2) that avoided blood vessels, portal tracts, and focal lesions was used. Three images that appeared subjectively consistent and to have minimal artifact were selected for each of the three nonbiopsy sites, and nine images were selected from the biopsy site for the placement of regions of interest. In this fashion, a total of 18 SWE values were obtained. Mean and

median elasticity values were calculated for each of the four measurement sites. All 18 elastograms were not available for 32 of the 136 patients (23.5%), and means and medians were calculated from the data available.

Liver Biopsy

Nonfocal liver biopsy was performed under US guidance by fellows in the department of abdominal imaging under the supervision of an attending physician with a minimum of 3 years of experience (range, 3–30 years). The patient gave consent and was given local anesthesia before the procedure. All biopsy specimens were obtained from the right lobe by using a 16-gauge full core biopsy instrument (BioPince; Medical Device Technologies, Gainesville, Fla). The quantity of tissue obtained was not routinely recorded at the time of biopsy; however, it is our divisional protocol to try to obtain at least one 16-gauge 2-cm-long core biopsy from the right lobe of the liver. All biopsy specimens were fixed in formalin and embedded in paraffin.

Histologic Examination

A subspecialist pathologist (A.K.B.) with 29 years of experience who was blinded to the SWE values and clinical information reviewed the biopsy specimens. The length of each biopsy specimen (in millimeters) and the number of portal tracts visualized were recorded. Visualization of a minimum of three portal triads and a biopsy sample at least 1 cm long were considered adequate for histologic examination. Liver fibrosis was staged by using the METAVIR staging system (17). Fibrosis, steatosis, and necroinflammatory scores obtained with the METAVIR scoring system were used for statistical analysis. In the METAVIR system, fibrosis is graded with a five-point ordinal scale ranging from 0 to 4 (F0, absent; F1, enlarged fibrotic portal tract; F2, few portal-portal septa but intact architecture; F3, many septa with architectural distortion but no obvious cirrhosis; and F4, cirrhosis). Steatosis was classified as absent (S0), less than 5% (S1), 5%–33% (S2), 34%–66% (S3), and more than 66% (S4). The necroinflammatory score was calculated on the basis of the METAVIR score for *(a)* piecemeal and/or interface hepatitis (score, 0–3) and *(b)* lobular hepatitis (score, 0–2) to provide a total necroinflammatory activity score of 0–3 (also classified as A0–A3) (17).

Statistical Analysis

Statistical analysis was performed with SPSS software (IBM SPSS, version 22.0; IBM, Armonk, NY). Mean SWE estimates of the Young modulus were calculated for each of the four liver SWE sites. The nonparametric Spearman correlation test was performed to identify the site with the highest positive correlation with the fibrosis, steatosis, and total necroinflammatory score determined with the METAVIR system. Confidence intervals (CIs) for the correlation were calculated by using an online CI generator (*http://vassarstats.net/rho.html*). The diagnostic performance of SWE in differentiating *(a)* fibrosis of less than F2 from fibrosis of F2 or greater, *(b)* fibrosis of less than F3 from fibrosis of F3 or greater, and *(c)* fibrosis of less than F4 from fibrosis of F4 was calculated by plotting receiver operating characteristic (ROC) curves by using the SWE values from the site of highest correlation to obtain the area under the ROC curve (AUC). Optimal cutoffs were used to evaluate sensitivity, specificity, positive predictive value, negative predictive value, positive likelihood ratio, and negative likelihood ratio, as calculated by using an online generator (*http://vassarstats.net/clin1.html*). The same sets of statistics were then repeated after omitting transplant recipients and for the subset of patients with HCV. Adjustment to minimize spectrum bias was also performed (Appendix E1 [online]).

Results

One hundred fifty patients were enrolled in the study between January 2010 and March 2013. SWE data could not be obtained at the biopsy site after insertion of the biopsy needle in nine patients. In all of these cases, the biopsy procedure could not be interrupted for SWE acquisition owing to patient discomfort. SWE data were not adequately acquired in two patients owing to obesity. Two patients were excluded because they did not meet the histologic examination criteria of a 10-mm-long specimen and a minimum of three portal triads. In one patient, the biopsy specimen was obtained from the left lobe; hence, this patient was excluded from the data analysis. The remaining 136 patients were included in the statistical analysis.

Table 1

Patient Demographics and Clinical Indication for Liver Biopsy

Demographic and Histologic Characteristics	No. of Patients (n = 136)
Sex	
M	70
F	66
Reason for biopsy	
Follow-up of known liver disease	72
Chronic HCV	43
Autoimmune hepatitis	18
HBV	8
Hemochromatosis	1
HIV and HCV coinfection	1
Alcoholic liver disease	1
Elevated liver function test	60
Elevated liver function test after transplantation	4
History of HCV	2
History of HIV and HCV coinfection	1
History of alcoholic liver disease	1

Note.—Data are numbers of patients. Male patients ranged in age from 18 to 72 years (mean, 47 years ± 13.02) and female patients ranged in age from 22 to 74 years (mean, 51 years ± 10.82) (P = .14). HBV = hepatitis B virus, HIV = human immunodeficiency virus.

Demographics

Among the 136 patients, there were 70 men and 66 women with a mean age of 49 years (range, 18–74 years). Liver biopsy was performed to evaluate *(a)* known liver disease (72 of 136 patients, 53%), *(b)* elevated liver function tests (60 of 136 patients, 44%), and *(c)* elevated liver function tests after liver transplantation (four of 136 patients, 3%) (Table 1).

The mean length of the histologic sample obtained at liver biopsy (±standard deviation) was 26 mm ± 8 (range, 10–53 mm), and the mean number of portal tracts was 13 ± 4.7 (range, 3–26). In 101 of the 136 patients (74%), the core biopsy sample was larger than 20 mm. In 107 of the 136 patients (79%), at least 10 portal tracts were visible. Most patients (82 of 136 patients, 60.3%) had stage F1 fibrosis at histologic examination. Stage S1 steatosis was the most common, occurring in 37 of the 136 patients (27.2%). Seventy-eight of the 136 patients (57.4%) had a necroinflammatory score of A1 (Table 2).

Spearman Correlation

Mean SWE values at all sites except those from the left lobe showed a significant correlation ($P < .05$) with fibrosis stage (r values are summarized in Table 3). Mean SWE values at the right upper lobe showed the highest correlation (r = 0.41; 95% CI: 0.26, 0.54). Steatosis stage had a weak correlation with SWE values of the left lobe (r = 0.24; 95% CI: 0.08, 0.4; P = .004) but did not correlate with SWE values at the right upper lobe (r = 0.45, P = .06), lower right lobe (r = 0.26, P = .09), and biopsy site (r = 0.04, P = .62). The total necroinflammatory score did not have a statistically significant correlation with SWE values at any of the four sites (Table 3).

Upper Right Lobe SWE Values

Table 4 summarizes the SWE estimates of the Young modulus at the right upper lobe site for each fibrosis stage, and Figure 2 displays the data as a box-and-whisker plot.

ROC Curves

The ROC curve (Fig 3) drawn to differentiate fibrosis stage of at least F2 (n = 35) from fibrosis stage of less than F2 (n = 101) by using SWE values at the right upper lobe provided an AUC of 0.77 (95% CI: 0.68, 0.86), with an optimal

Table 2

Summary of Fibrosis, Steatosis, and Necroinflammatory Stages

Parameter	No. of Patients (n = 136)
Fibrosis	
F0	19 (14)
F1	82 (60.3)
F2	18 (13.2)
F3	10 (7.4)
F4	7 (5.1)
Steatosis	
S0	35 (25.7)
S1	37 (27.2)
S2	27 (19.8)
S3	31 (22.8)
S4	6 (4.4)
Necroinflammation	
A0	23 (16.9)
A1	78 (57.4)
A2	24 (17.6)
A3	11 (8.1)

Note.—Histologic findings were evaluated with METAVIR criteria. Numbers in parentheses are percentages.

Table 3

Correlation of SWE Values at Different Sites with Fibrosis, Steatosis, and Necroinflammation

	Fibrosis			Steatosis			Necroinflammation		
Site	*P* Value	*r* Value	95% CI	*P* Value	*r* Value	95% CI	*P* Value	*r* Value	95% CI
Left lobe	.061	0.16	−0.01, 0.32	.004	0.24	0.08, 0.40	.61	0.04	−0.21, 0.13
Upper right lobe	<.001	0.41	0.26, 0.54	.449	0.07	−0.10, 0.23	.191	0.11	0.02, 0.35
Lower right lobe	<.001	0.35	0.19, 0.49	.256	0.10	−0.71, 0.26	.418	0.07	−0.10, 0.24
Biopsy site	.009	0.23	0.06, 0.38	.624	0.04	0.13, 0.21	.581	0.05	0.36, 0.62

Note.—Data were obtained with the Spearman correlation.

Table 4

Summary of SWE Values from Right Upper Lobe according to Fibrosis Stage in All Patients and in the Subset with HCV

	All Patients					Patients with HCV*			
Parameter	F0 (n = 19)	F1 (n = 82)	F2 (n = 18)	F3 (n = 10)	F4 (n = 7)	F1 (n = 31)	F2 (n = 5)	F3 (n = 6)	F4 (n = 2)
Median	6.66	7.29	8.42	9.64	9.80	6.87	9.02	9.53	11.78
Standard deviation	1.80	2.11	2.01	1.40	2.37	2.24	1.48	1.48	3.06
Minimum	4.70	3.36	3.95	7.83	7.62	4.25	7.3	7.93	9.61
Maximum	10.58	12.54	12.23	11.97	13.94	12.09	11.20	11.97	13.94
1st Quartile	5.11	5.72	7.57	8.20	8.94	5.60	7.65	8.20	9.61
3rd Quartile	8.04	8.50	10.16	10.72	13.62	9.33	10.17	10.88	…
Outlier	…	…	…	…	…	…	1	…	…

Note.—All data are given in kilopascals.

* None of the patients with HCV had stage F0 fibrosis.

cutoff of 7.29 kPa (sensitivity = 91.4%, specificity = 52.5%). AUCs for differentiating fibrosis stage of at least F3 (n = 17) from fibrosis stage of less than F3 (n = 119) and stage F4 fibrosis (n = 7) from fibrosis of less than F4 (n = 129) were 0.82 (95% CI: 0.75, 0.91) and 0.82 (95% CI: 0.69, 0.95), respectively.

Table 5 summarizes observed AUC values, sensitivity, specificity, positive predictive value, negative predictive value, positive likelihood ratio, and negative likelihood ratio for optimal cutoff values for each of the ROC curves (Fig 4).

When liver transplant recipients (n = 4) were omitted from the analysis, the observed AUCs were 0.78 (95% CI: 0.69, 0.86) for the diagnosis of fibrosis stage of at least F2 and 0.83 (95% CI: 0.76, 0.91) and 0.82 (95% CI: 0.70, 0.95) for the diagnosis of fibrosis stage of F3 or greater or F4.

Patients with Chronic HCV

Forty-four patients (male-to-female ratio, 32:12) had a history of HCV without liver transplantation (mean age, 52 years ± 9; range, 25–65 years). Table 4 summarizes the SWE values from the upper right lobe for each fibrosis stage in all patients and in patients with HCV; Figure 4 displays that data in the form of a box-and-whisker plot.

An ROC curve (Fig 5) drawn to differentiate fibrosis stage of at least F2 (n = 13) from fibrosis stage of less than F2 (n = 31) with use of SWE values at the right upper lobe provided an AUC of 0.80 (95% CI: 0.68, 0.92), with an optimal cutoff of 7.25 kPa (sensitivity = 100%, specificity = 58.1%). AUCs for differentiating fibrosis stage of F3 or greater (n = 8) from fibrosis stage of less than F3 (n = 36) and stage F4 fibrosis (n = 2) from fibrosis stage of less than F4 (n = 32) were 0.82 (95% CI: 0.70, 0.95) and 0.89 (95% CI: 0.73, 1.00), respectively.

Correction for ROC Curves

The difference between the mean fibrosis stage of advanced fibrosis and the mean fibrosis stage of nonadvanced fibrosis (DANA) for our patient cohort was 1.87; hence, the adjusted AUC for differentiating advanced fibrosis from nonadvanced fibrosis was 0.84. Adjusted AUC values obtained from a DANA correction of 1.87 are summarized in Table 6, along with observed ROC values.

The calculated DANA for the subset of patients with HCV was 1.77. The adjusted AUC for differentiating advanced fibrosis from nonadvanced fibrosis was 0.87 (95% CI: 0.74, 1.00).

Discussion

In this prospective cross-sectional study, we estimated the diagnostic accuracy of SWE for liver fibrosis estimation in patients with CLD and HCV when using liver biopsy as the standard of reference and evaluated the optimal region from which to obtain measurements.

In our study, upper right lobe SWE Young modulus estimates showed the highest correlation with fibrosis stage (r = 0.41). Although the mean lower right

Figure 2

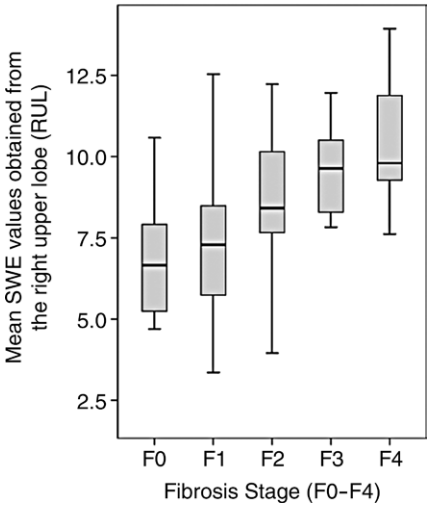

Figure 2: Box-and-whisker plot shows mean SWE values at upper right lobe for various fibrosis stages. Central box represents values from 25th to 75th quartile, and line in middle of box is the median. Error bars show minimum and maximum values.

Figure 3

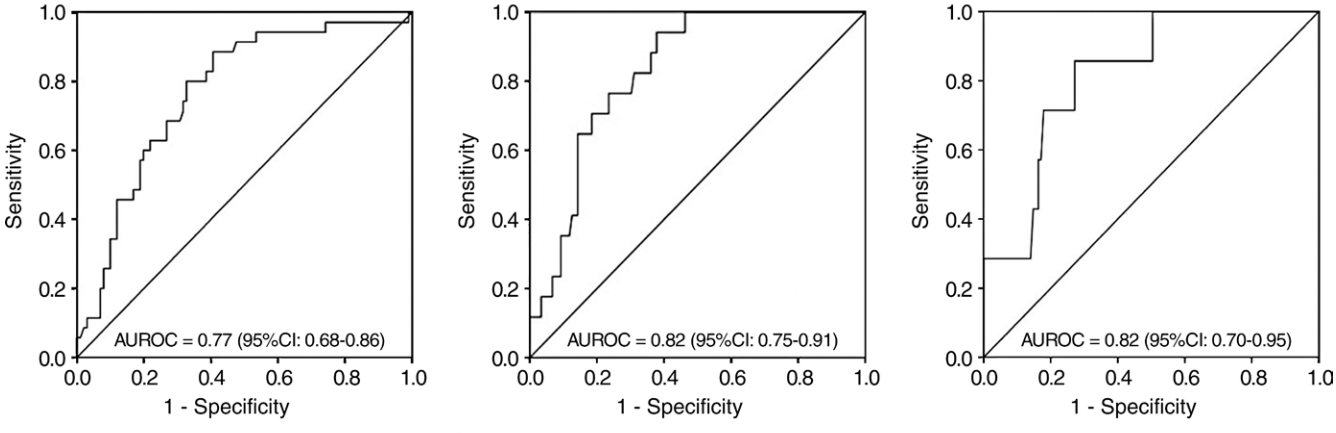

Figure 3: Graphs show AUCs (*AUROC*) for mean SWE values at upper right lobe to differentiate **(a)** fibrosis stage of at least F2 from fibrosis stage of less than F2, **(b)** fibrosis stage of at least F3 from fibrosis stage of less than F3, and **(c)** fibrosis stage of F4 from fibrosis stage of less than F4.

Table 5

Diagnostic Performance of SWE

Parameter	≥F2	≥F3	F4
Observed AUC	0.77 (0.68, 0.86)	0.82 (0.75, 0.91)	0.82 (0.70, 0.95)
Optimal cutoff value (kPa)	7.29	8.90	9.59
Sensitivity (%)	91.4 (75.6, 97.8) [32/35]	76.5 (49.8, 92.2) [13/17]	71.4 (30.3, 94.9) [5/7]
Specificity (%)	52.5 (42.3, 62.4) [53/101]	76.5 (67.6, 83.6) [91/119]	82.2 (74.2, 88.1) [106/129]
PPV (%)	40.0 (29.4, 51.6) [32/80]	31.7 (18.6, 48.2) [13/41]	17.9 (6.8, 37.6) [5/28]
NPV (%)	94.6 (84.2, 98.6) [53/56]	95.8 (88.9, 98.6) [91/95]	98.1 (92.8, 99.7) [106/108]
Positive LR	1.92 (1.53, 2.41)	3.25 (2.14, 4.93)	4.01 (2.20, 7.28)
Negative LR	0.16 (0.05, 0.49)	0.31 (0.13, 0.73)	0.35 (0.11, 1.13)

Note.—Numbers in parentheses are 95% CIs. Numbers in brackets are raw data. LR = likelihood ratio, NPV = negative predictive value, PPV = positive predictive value.

Figure 4

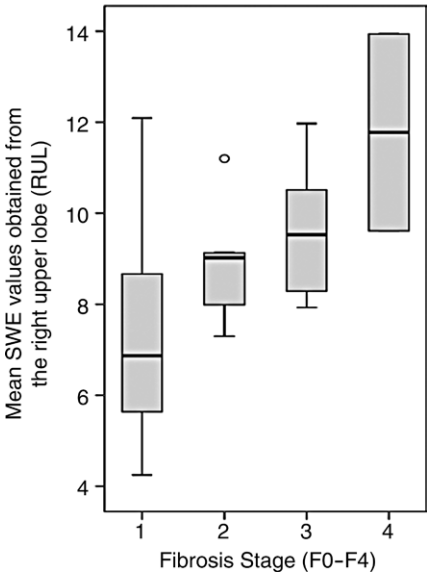

Figure 4: Box-and-whisker plot shows mean SWE values at upper right lobe for various fibrosis stages in patients with HCV. Central box represents values from 25th to 75th quartile, and line in middle of box is the median. Error bars show minimum and maximum values. ○ = outlier.

lobe and biopsy site SWE values also showed correlation, there was no correlation between fibrosis stage and mean SWE values in the left lobe. Steatosis correlated with mean SWE values in the left lobe, but SWE values at other sites did not correlate with steatosis or total necroinflammatory score. Friedrich-Rust et al (18) found no difference between the correlation of left and right lobe acoustic radiation force imaging measurements with fibrosis, but showed that right lobe values provided a higher AUC for diagnosing fibrosis stage of at least F2 and at least F3 (but a higher AUC for stage F4 fibrosis assessment with values obtained from the left lobe). It is unclear why our results differ in this regard from those reported by Friedrich-Rust et al (18). Nonetheless, our results appear consistent in that the right upper lobe was consistently the superior site.

In our study, steatosis was correlated with SWE measurements at the left liver lobe only. The reason for this is unclear. The literature is inconsistent regarding the effects of steatosis and necroinflammation on fibrosis assessment. Some studies with transient elastography (19–21), SWE (21), and MR elastography (22,23) have concluded that the correlation between liver stiffness values and fibrosis stage is not affected by steatosis or necroinflammation. Other studies have suggested that inflammation, as suggested by elevated transaminase levels (24,25) or diagnosed at liver biopsy (26–28), affects transient elastography assessment of fibrosis. Similarly, steatosis has been reported to have no effect on acoustic radiation force imaging–based fibrosis assessment (29), whereas in several transient elastography studies, steatosis has been reported to have an effect on noninvasive fibrosis staging (28,30,31). It is possible our finding of correlation between liver steatosis and SWE liver stiffness estimates in the left lobe represents a type I error.

In the entire subject population, the AUC for differentiating nonadvanced fibrosis (F0–F1) from advanced fibrosis (F2–F4) was 0.77 ($P < .001$). This was adjusted to 0.84 after applying the DANA correction to minimize spectrum bias. The observed and adjusted AUCs for differentiating nonadvanced fibrosis (F0–F1) from advanced fibrosis (F2–F4) in patients with chronic HCV were 0.80 and 0.87, respectively. Observed AUCs for differentiating severe fibrosis (≥F3) were the same in patients with CLD and those with HCV (AUC = 0.82), whereas the observed AUCs for the differentiation of cirrhosis (F4) were 0.82 in patients with CLD and 0.89 in those with HCV. Removal of the liver transplant recipients from the sample had little effect on the observed AUC, which was 0.78 for the diagnosis of fibrosis stage of at least F2 and unchanged for the diagnosis of fibrosis stage of at least F3 or at least F4.

Previous research has studied SWE liver fibrosis staging in patients with CLD (32), patients with HCV (21), and patients with hepatitis B (33). Although Bavu et al (32) do not describe the cause of liver disease in their patient cohort or the method they used to grade fibrosis, the observed AUC for SWE in our study (AUC = 0.77) was lower than that in their study (AUC = 0.95). When comparing the subset of patients with HCV in our cohort, the observed AUC of 0.80 is also lower than the 0.92 AUC obtained by Ferraioli et al (21). Because Ferraioli et al do not describe the breakdown of patients with stage F0 and F1 fibrosis in their patient cohort and have not adjusted for spectrum bias, it is unclear as to what extent our results differ from theirs.

Figure 5

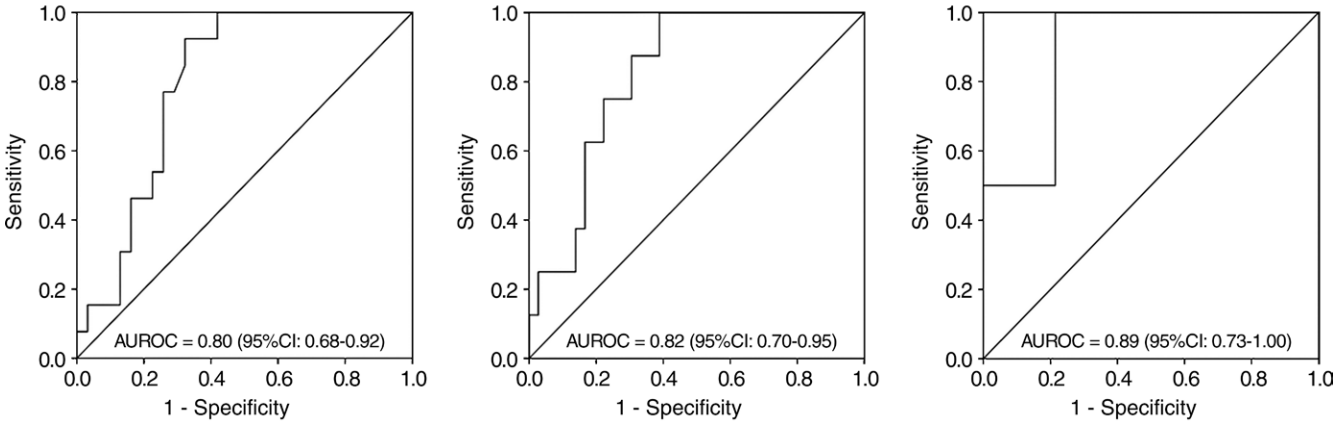

Figure 5: Graphs show AUCs (*AUROC*) for mean SWE values at upper right lobe to differentiate **(a)** fibrosis stage of F2 or greater from fibrosis stage of less than F2, **(b)** fibrosis stage of F3 or greater from fibrosis stage of less than F3, and **(c)** fibrosis stage of F4 from fibrosis stage of less than F4 in patients with HCV.

Table 6

Comparison of AUCs for All Patients and the Subset of Patients with HCV

Fibrosis Stage and AUC Type	All Patients	Patients with HCV
F2		
Observed AUC	0.77 (0.68, 0.86)	0.80 (0.68, 0.92)
Adjusted AUC	0.84	0.87
F3: Observed AUC	0.82 (0.75, 0.91)	0.82 (0.70, 0.95)
F4: Observed AUC	0.82 (0.70, 0.95)	0.89 (0.73, 1.0)

Note.—Numbers in parentheses are 95% CIs.

The differentiation of nonadvanced (F0 and F1) and advanced (F2–F4) fibrosis is particularly relevant in HCV, where advanced fibrosis at the time of diagnosis has been shown to correlate with long-term cirrhosis risk (34–37). In our study, the observed AUC and adjusted AUC for the diagnosis of advanced fibrosis are high, which suggests that SWE may be useful to answer this clinically relevant question. However, it is also important to note that SWE estimates of liver elasticity at given fibrosis stages show substantial degrees of overlap. As a result, we do not recommend that these presently be used to assign a specific fibrosis stage to each patient.

Our study has limitations. First, our patients had a range of liver diseases. Although all follow the common pathway of progressive fibrosis culminating in cirrhosis, it is known that fibrosis patterns differ among diseases. This variation may produce heterogeneous liver elasticity measurements. Second, a relatively small number of our patients had advanced fibrosis. Although we have used the DANA correction to minimize spectrum bias, it would have been preferable to have more subjects with advanced fibrosis. Finally, we used the METAVIR staging system for liver fibrosis. This staging system was originally designed for viral hepatitis, whereas causes of liver disease in our sample population extended beyond viral hepatitis. Nonetheless, the clear correlation between liver elasticity estimates and fibrosis stage demonstrates that this approach is likely valid.

We conclude that estimates of the Young modulus obtained with SWE in the upper right lobe of the liver can be used to differentiate advanced fibrosis (≥F2) from nonadvanced fibrosis.

Our study does not show any effect of steatosis or inflammation on the fibrosis estimation with use of SWE; however, given that the published literature is contradictory, larger studies are needed to define the effect of these and other confounders and to establish SWE thresholds for various fibrosis stages in distinct diffuse liver diseases.

Acknowledgments: SuperSonic Imagine supported the study by loaning an Aixplorer system to the investigators. We acknowledge Jingwen Chen, MD, RDMS, who performed shear-wave elastography.

Disclosures of Conflicts of Interest: **A.E.S.** disclosed no relevant relationships. **M.D.** disclosed no relevant relationships. **A.V.** disclosed no relevant relationships. **A.K.B.** disclosed no relevant relationships. **E.F.H.** Activities related to the present article: disclosed no relevant relationships. Activities not related to the present article: is a paid consultant for Hologic; receives payment for lectures including service on speakers bureaus from Cambridge Healthtech. Other relationships: disclosed no relevant relationships. **J.M.** disclosed no relevant relationships. **K.E.C.** Activities related to the present article: disclosed no relevant relationships. Activities not related to the present article: is a paid consultant for Gilead. Other relationships: disclosed no relevant relationships. **R.T.C.** disclosed no relevant relationships.

References

1. Younossi ZM, Stepanova M, Afendy M, et al. Changes in the prevalence of the most common causes of chronic liver diseases in

the United States from 1988 to 2008. Clin Gastroenterol Hepatol 2011;9(6):524–530. e1; quiz e60.

2. Bell BP, Manos MM, Zaman A, et al. The epidemiology of newly diagnosed chronic liver disease in gastroenterology practices in the United States: results from population-based surveillance. Am J Gastroenterol 2008;103(11):2727–2736; quiz 2737.
3. Sebastiani G, Castera L, Halfon P, et al. The impact of liver disease aetiology and the stages of hepatic fibrosis on the performance of non-invasive fibrosis biomarkers: an international study of 2411 cases. Aliment Pharmacol Ther 2011;34(10):1202–1216.
4. Alberti A, Vario A, Ferrari A, Pistis R. Review article: chronic hepatitis C—natural history and cofactors. Aliment Pharmacol Ther 2005;22(Suppl 2):74–78.
5. Clark JM, Diehl AM. Nonalcoholic fatty liver disease: an underrecognized cause of cryptogenic cirrhosis. JAMA 2003;289(22): 3000–3004.
6. de Franchis R, Hadengue A, Lau G, et al. EASL International Consensus Conference on Hepatitis B. 13–14 September, 2002 Geneva, Switzerland. Consensus statement (long version). J Hepatol 2003;39(Suppl 1):S3–S25.
7. Regev A, Berho M, Jeffers LJ, et al. Sampling error and intraobserver variation in liver biopsy in patients with chronic HCV infection. Am J Gastroenterol 2002;97(10):2614–2618.
8. Schmeltzer PA, Talwalkar JA. Noninvasive tools to assess hepatic fibrosis: ready for prime time? Gastroenterol Clin North Am 2011;40(3):507–521.
9. Ronot M, Asselah T, Paradis V, et al. Liver fibrosis in chronic hepatitis C virus infection: differentiating minimal from intermediate fibrosis with perfusion CT. Radiology 2010;256(1):135–142.
10. Hagiwara M, Rusinek H, Lee VS, et al. Advanced liver fibrosis: diagnosis with 3D whole-liver perfusion MR imaging—initial experience. Radiology 2008;246(3):926–934.
11. Wang QB, Zhu H, Liu HL, Zhang B. Performance of magnetic resonance elastography and diffusion-weighted imaging for the staging of hepatic fibrosis: A meta-analysis. Hepatology 2012;56(1):239–247.
12. Bonekamp S, Torbenson MS, Kamel IR. Diffusion-weighted magnetic resonance imaging for the staging of liver fibrosis. J Clin Gastroenterol 2011;45(10):885–892.
13. Friedrich-Rust M, Ong MF, Martens S, et al. Performance of transient elastography for the staging of liver fibrosis: a meta-analysis. Gastroenterology 2008;134(4):960–974.
14. Friedrich-Rust M, Nierhoff J, Lupsor M, et al. Performance of acoustic radiation force impulse imaging for the staging of liver fibrosis: a pooled meta-analysis. J Viral Hepat 2012;19(2):e212–e219.
15. Chon YE, Choi EH, Song KJ, et al. Performance of transient elastography for the staging of liver fibrosis in patients with chronic hepatitis B: a meta-analysis. PLoS ONE 2012;7(9):e44930.
16. Bercoff J, Tanter M, Fink M. Supersonic shear imaging: a new technique for soft tissue elasticity mapping. IEEE Trans Ultrason Ferroelectr Freq Control 2004;51(4):396–409.
17. Bedossa P, Poynard T. An algorithm for the grading of activity in chronic hepatitis C. The METAVIR Cooperative Study Group. Hepatology 1996;24(2):289–293.
18. Friedrich-Rust M, Romen D, Vermehren J, et al. Acoustic radiation force impulse imaging and transient elastography for non-invasive assessment of liver fibrosis and steatosis in NAFLD. Eur J Radiol 2012;81(3):e325–e331.
19. Sandrin L, Fourquet B, Hasquenoph JM, et al. Transient elastography: a new noninvasive method for assessment of hepatic fibrosis. Ultrasound Med Biol 2003;29(12):1705–1713.
20. Castéra L, Vergniol J, Foucher J, et al. Prospective comparison of transient elastography, fibrotest, APRI, and liver biopsy for the assessment of fibrosis in chronic hepatitis C. Gastroenterology 2005;128(2):343–350.
21. Ferraioli G, Tinelli C, Dal Bello B, et al. Accuracy of real-time shear wave elastography for assessing liver fibrosis in chronic hepatitis C: a pilot study. Hepatology 2012;56(6):2125–2133.
22. Wong VW, Vergniol J, Wong GL, et al. Diagnosis of fibrosis and cirrhosis using liver stiffness measurement in nonalcoholic fatty liver disease. Hepatology 2010;51(2):454–462.
23. Huwart L, Sempoux C, Vicaut E, et al. Magnetic resonance elastography for the noninvasive staging of liver fibrosis. Gastroenterology 2008;135(1):32–40.
24. Coco B, Oliveri F, Maina AM, et al. Transient elastography: a new surrogate marker of liver fibrosis influenced by major changes of transaminases. J Viral Hepat 2007;14(5): 360–369.
25. Oliveri F, Coco B, Ciccorossi P, et al. Liver stiffness in the hepatitis B virus carrier: a noninvasive marker of liver disease influenced by the pattern of transaminases. World J Gastroenterol 2008;14(40):6154–6162.
26. Vispo E, Barreiro P, Del Valle J, et al. Overestimation of liver fibrosis staging using transient elastography in patients with chronic hepatitis C and significant liver inflammation. Antivir Ther 2009;14(2):187–193.
27. Kim SU, Kim JK, Park YN, Han KH. Discordance between liver biopsy and Fibroscan in assessing liver fibrosis in chronic hepatitis b: risk factors and influence of necroinflammation. PLoS ONE 2012;7(2):e32233.
28. Fraquelli M, Rigamonti C, Casazza G, et al. Etiology-related determinants of liver stiffness values in chronic viral hepatitis B or C. J Hepatol 2011;54(4):621–628.
29. Fierbinteanu-Braticevici C, Andronescu D, Usvat R, Cretoiu D, Baicus C, Marinoschi G. Acoustic radiation force imaging sonoelastography for noninvasive staging of liver fibrosis. World J Gastroenterol 2009;15(44):5525–5532.
30. Sánchez-Conde M, Montes Ramírez ML, Bellón Cano JM, et al. Impact of liver steatosis on the correlation between liver stiffness and fibrosis measured by transient elastography in patients coinfected with human immunodeficiency virus and hepatitis C virus. J Viral Hepat 2011;18(7):e278–e283.
31. Kim SU, Kim Y, Ahn SH, et al. The impact of steatosis on liver stiffness measurement in patients with chronic hepatitis B. Hepatogastroenterology 2010;57(101):832–838.
32. Bavu E, Gennisson JL, Couade M, et al. Noninvasive in vivo liver fibrosis evaluation using supersonic shear imaging: a clinical study on 113 hepatitis C virus patients. Ultrasound Med Biol 2011;37(9):1361–1373.
33. Leung VY, Shen J, Wong VW, et al. Quantitative elastography of liver fibrosis and spleen stiffness in chronic hepatitis B carriers: comparison of shear-wave elastography and transient elastography with liver biopsy correlation. Radiology 2013;269(3):910–918.
34. Kato Y, Nakata K, Omagari K, et al. Risk of hepatocellular carcinoma in patients with cirrhosis in Japan. Analysis of infectious hepatitis viruses. Cancer 1994;74(8):2234–2238.
35. Takano S, Yokosuka O, Imazeki F, Tagawa M, Omata M. Incidence of hepatocellular carcinoma in chronic hepatitis B and C: a prospective study of 251 patients. Hepatology 1995;21(3):650–655.
36. Yamada G, Tanaka E, Miura T, et al. Epidemiology of genotypes of hepatitis C virus in Japanese patients with type C chronic liver diseases: a multi-institution analysis. J Gastroenterol Hepatol 1995;10(5):538–545.
37. Di Bisceglie AM. Hepatitis C and hepatocellular carcinoma. Semin Liver Dis 1995; 15(1):64–69.